Effect of DNAJB6 on α-synuclein amyloid fibril aggregation and dis-aggregation

Josef Getachew

LUND
UNIVERSITY

Department of biochemistry and structural biology

Supervisor: Sara Linse

Deputy supervisors: Lei Ortigosa, Emil Axell, Max Lindberg

Examiner: Kristine Steen Jensen

June 2023

Abstract

Amyloid proteins are a group of proteins with the ability to form large fibrillar aggregates, identifiable by their cross-β core structure. These aggregates are linked to several different neurodegenerative diseases such as Parkinson's disease and Alzheimer's disease and due to the growing rate of people diagnosed, there is a need to combat these diseases. Aggregation of amyloid proteins is caused by the misfolding of nascent protein. The human body, however, has a machinery to prevent this, through a protein class known as chaperones. They are defined as protein which can prevent misfolding or aggregation of other protein. One chaperone from the Hsp40 class, DNAJB6, has been shown to prevent aggregation of amyloid protein. An attempt to describe the thermodynamic background behind this phenomena has been done by Linse et al. (2021), with the "unhappy chaperone" hypothesis [1]. Through the formation of co-aggregates between chaperones and amyloid protein, there is a lowering of the free energy of the system, leading to an increase in solubility for the amyloid protein. An increase in solubility is only possible through an increase in free energy for the amyloid protein, however this is offset by a larger decrease for the chaperone. The decrease in free energy for the chaperone when forming co-aggregates explains the "unhappiness" of chaperones to be free in solution.

The aim of this project was to exhibit this increase in solubility for the amyloid protein α-synuclein, whose aggregation is the cause of Parkinson's disease. DNAJB6 was the chosen chaperone, and the goal was to determine if an increase in solubility is a true thermodynamic equilibrium, which means this effect should lead to the same solubility both from a system consisting of 100% monomeric α-synuclein or 100% fibrillar α-synuclein. Also, there was prior method development for how to best measure the monomer concentration.

α-synuclein aggregation at 37° C and pH 5.5, was measured both without DNAJB6 and with 1% DNAJB6, this was done through a developed HPLC absorbance protocol and OPA fluorescence. Possible α-synuclein disaggregation was also investigated on samples with aggregated α-synuclein, where 1% and 10% DNAJB6 was added, these also measured with HPLC and OPA. α-synuclein solubility were furthermore also measured with NMR, and DNAJB6 was also added here, at the end of fibrillization to detect possible dis-aggregation.

From the results, the following conclusions could be determined. α-synuclein solubility was determined to be 0.39 $\pm$0.016 μM measured with OPA, and 0.11 $\pm$0.013 μM, measured with HPLC. Aggregation in the presence of 1% DNAJB6 lead to delayed aggregation and possible increase in solubility. With SDS-PAGE and MALDI, the formation of aggregates consisting of both α-synuclein and DNAJB6 was identified. Dis-aggregation was not observed and could be attributed to the low solubility of DNAJB6 at pH 5.5. HPLC was determined to be a sensitive and accurate system for measuring α-synuclein monomer concentration, but further development should be done to improve robustness and reproducibility. Lastly, NMR was determined as a viable method for measuring α-synuclein solubility at pH 5.5, although it is not yet dependable for discontinuous measurements.

Acknowledgements

Firstly, I would like to thank my supervisor Sara Linse for the opportunity to work on this highly interesting and fun project, in an amazing group, and also for always lending your knowledge and your guidance. To Max, Emil and Lei, thank you for enduring my endless questions every day, for your support both in my current work but also in my future, and for at times putting my work ahead of yours, it has not gone unnoticed. Also, thank you to the rest of Sara Linse´s group at the department of biochemistry and structural biology (special thanks to Jelica Milosevic for providing purified DNAJB6).

Lastly, to my family, without you there would be no master thesis, there would be no masters degree, there would be nothing really. I owe it all to you and words can not describe my gratitude to you.

Contents

1 Introduction

Parkinson's disease is a neurodegenerative disease affecting 2-3% of the population above 65 years [2]. One of the believed underlying causes in the disease and other neurodegenerative diseases such as Alzheimer's disease is the aggregation and misfolding of protein, forming amyloid fibrils. In the 21st century, this group of diseases is rapidly growing with many of them first discovered just one or two generations ago [3]. One of the main symptoms, dementia, has been shown to increase exponentially with age [4]. As these diseases are often related to aging, the increase in the average age of the human population requires a need to understand neurodegenerative diseases and finding possible cures and countermeasures.

Amyloid fibrils are large protein aggregate assemblies, structurally identified by their shared core of cross-β-sheets and their ability to stain Congo red and being ThT positive. In the specific case of Parkinson's disease, it is the protein α-synuclein which aggregates [5]. The aggregation of α-synuclein leads to the formation of insoluble structures known as Lewy bodies in neurons of patients with neurodegenerative diseases. While it has not been shown what the direct correlation between fibrillated protein and these diseases is, it has been suggested that the oligomeric intermediaries formed on the way to fibrillization are the most toxic species in the pathway, as opposed to the fibrils [6]. α-synuclein, is an intrinsically disordered protein, meaning it has a random coil. This property of α-synuclein makes it more prone to misfolding. Upon binding to lipid membranes, however, α-synuclein adopts a helical conformation [7].

Due to the increasing amount of people diagnosed with neurodegenerative diseases, there are significant efforts trying to understand and combat misfolding and aggregation of amyloid proteins. One highly interesting process is the action of chaperones. Chaperones are a family of proteins which are involved in the folding mechanism of proteins, acting as a safeguard against misfolding. There are many different chaperones and they can vary in terms of structure and in their individual function [8]. In a study by Gao et al. (2015), a three-chaperone system showed highly effective dissolution of α-synuclein fibrils [9]. Effectiveness was dependent on the amount and presence of each chaperone.

To understand the mechanisms behind chaperones ability to prevent aggregation and misfolding, a recent article presented by Linse et al (2021) proposes a thermodynamic view of the ability of chaperones to increase the solubility of amyloid proteins [10]. Through the formation of co-aggregates with amyloid proteins, chaperones decrease their own chemical potential and the overall free energy for a given chaperone and amyloid protein system. Effectively increasing the solubility of the amyloid protein.

The aim of this work is to investigate the effect of DNAJB6 on the solubility of α-synuclein. Examining the thermodynamic effect of DNAJB6 in both the aggregation of monomeric α-synuclein as well as dis-aggregation of fibrillar α-synuclein. The hope is to reach the equilibrium point for α-synuclein in both reaction pathways as a means to determine a true thermodynamic equilibrium. Furthermore, there will be method development prior, to find the most optimal method to measure monomeric α-synuclein.

2 Background

2.1 Protein folding

The folding of proteins is a process where the protein attempt to reach its energetically most favorable state [11]. The two main factors determining the most favorable fold are energetic contribution from entropy and enthalpy. Entropy is the number of configurations a system can take and is easiest explained as the amount of freedom the protein as a net of all residues and the overall structure has.

Enthalpy is the total internal energy of the system, made up in part of the intramolecular bonds of the protein. These two factors are in balance with each other, and the most stable fold is that which has the overall lowest free energy as a function of entropy and enthalpy.

Proteins can structurally be described by which "state" they are in, the unfolded or native state. In the unfolded state they generally exhibit no tertiary structure and so are deemed unfolded whereas in the native state, the intramolecular contacts in the tertiary structure govern the fold described as the native state. It is in the native state proteins are considered functional. Although it would be simple to describe protein folding as only existing in the unfolded state and the folded native state, in reality there are several intermediary states on the pathway between these two states. As seen in figure 1 there are many different conformations the protein could take with a lower free energy than the unfolded state, and while they are larger than the native state, there is the possibility of the protein being kinetically trapped in certain conformation due to a high activation barrier preventing it from reaching a more favorable fold.

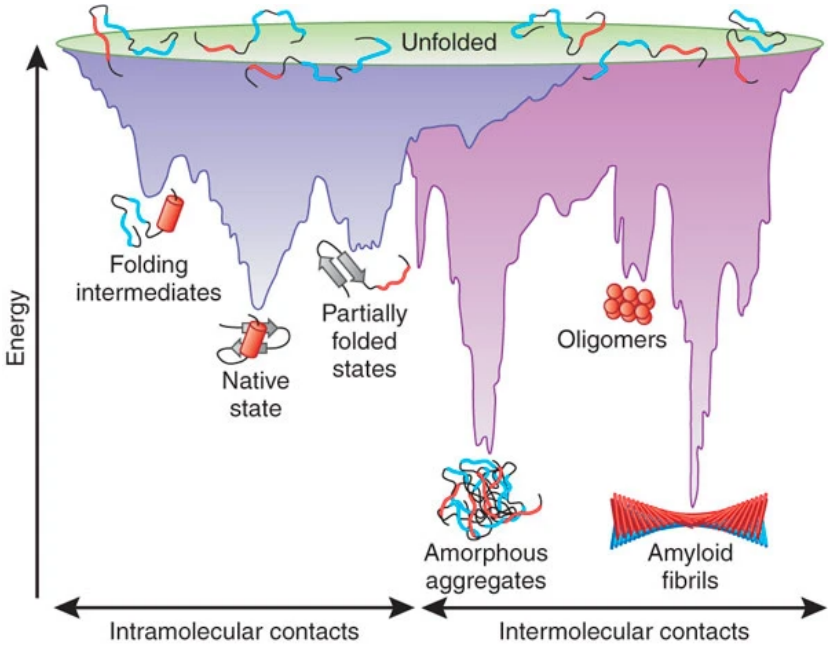

Figure 1: Folding states of amyloid proteins. [12]

2.2 Amyloid fibrils

Amyloid proteins are protein aggregates prone to form large fibrillar structures identified by their core of cross-β-sheets which are ordered perpendicular against the axis of the fibril [13]. Building these fibrils through intermolecular forces are monomeric proteins. The monomeric proteins involved in amyloid fibril formation, exhibit common motifs in their amino acid sequence, which are prone to form β-sheet structures. High hydrophobicity and rigidness are common properties in these motifs [13]. Amyloid fibrils are in most cases a result of misfolding of a native protein. Misfolding could lead to states which are amyloidogenic, prone to form nuclei such as an oligomeric intermediate state, eventually leading to large fibrils. As these nuclei grow, adding monomers, they can form proto-fibrils, longer, flexible oligomers. These can then adopt the further lengthened, cross-β ordered structures, referred to as proto-filaments [13]. It is these proto-filaments that form fibrils. Typically, fibrils are made up of 2-6 proto-filaments twisted around each other [13]. In figure 2, a cryo-EM density map of an α-synuclein

fibril is shown. The two protofilaments are colored in purple and yellow, with the length of a full pitch (360 °helical turn) determined as 239 nm. Also seen is the length of one monomer of α-synuclein along the axis of a protofilament, determined as 4.78 Å. Meaning there are 500 monomers building up one helical turn.

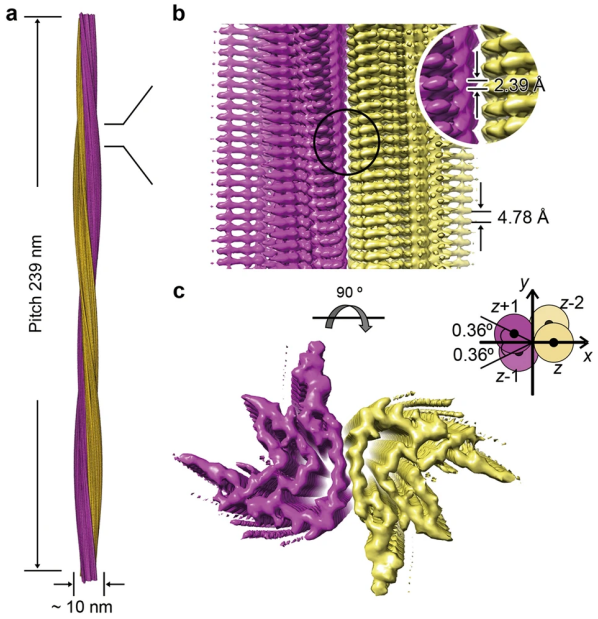

Figure 2: 3D density map of one example of a structure of a α-synuclein fibril composed of two protofilaments in purple and yellow captured through cryo-EM. [14]

The formation of amyloid fibrils can be divided into four processes, primary nucleation, elongation, secondary nucleation and fragmentation [13]. Primary nucleation is the process of nuclei formation, this can be divided into two types, homogeneous and heterogeneous primary nucleation. Homogeneous nucleation occurs in solution between two or more monomers of the same type, as opposed to heterogeneous, which happens on interfaces such as surfaces. Therefore, surfaces are believed to be highly impactful on aggregation kinetics [13]. Nuclei can be defined as the smallest oligomeric state for which further growth is more likely than dis-aggregation [13]. After the formation of nuclei, these can grow through elongation which is the addition of monomers to the ends of the growing fibrils. Important to note is how all these processes are reversible, meaning that as in the case of elongation, while monomers are added to the ends there are also monomers that leave. If the rate constants for the addition of monomers is larger than the removal of monomers and ratio of the concentrations of fibrils and monomers is lower than given by this ratio, growth occurs until equilibrium is reached. In the case of primary nucleation and elongation, both processes are concentration dependent.

Secondary nucleation is the formation of nuclei on the surface of already existing fibrils. Homogeneous nucleation is catalyzed on the sides (along fibril axis) of fibrils where monomers are added and eventually leaves the existing structure to form new fibrils [13]. As with primary nucleation and elongation, secondary nucleation is also concentration dependent. The final process, fragmentation, is the fragmentation of existing fibrils due to mechanical stress, thermal energy or by chaperones [13]. By dividing fibrils, there are more available ends for elongation to occur, leading to an increase in overall fibrillation rate of the system. The four processes are illustrated in figure 3. Typical aggregation kinetics can also be seen in figure 3. Although there is exponential growth in all phases, fibrils are not detected in the first phase, known as the lag phase [15]. Secondary nucleation and elongation leads to increased growth with a detectable exponential growth, until it reaches a plateau of fibril mass growth.

Amyloid "seeds" are already formed fibrils which can be used to promote aggregation of monomeric protein.

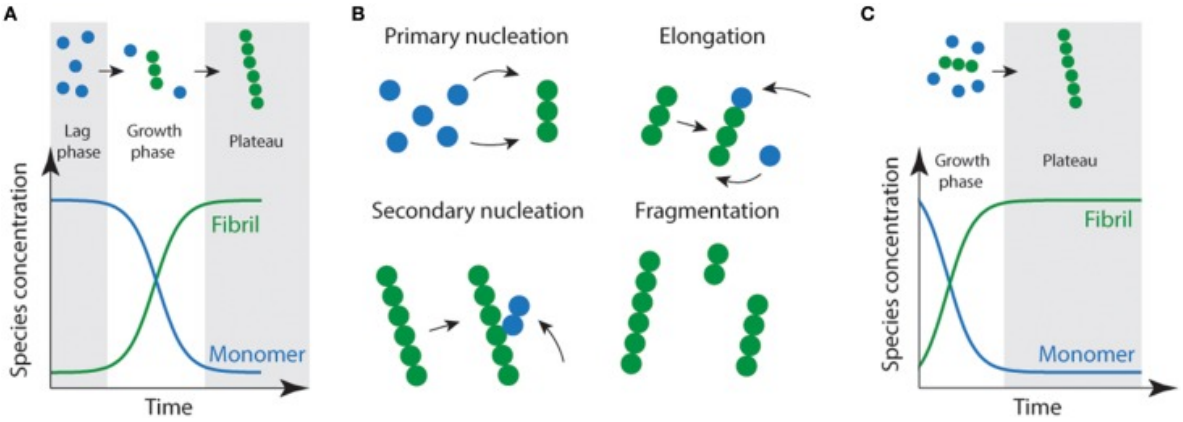

Figure 3: A) Typical aggregation kinetics, with a lag phase, exponential growth and a plateau. B) The four processes in amyloid fibril formation, primary nucleation, elongation, secondary nucleation and fragmentation, illustrated. C) Illustration of how the addition of seeds lead to a decreased lag phase. [16]

Although cross-β-sheets are found in fibrils of different proteins, such as α-synuclein or tau, the exact structures of the fibrils vary, even between two fibrils formed from the same monomeric protein. Amyloid fibrils are polymorphous, identical monomers can form different structures. The polymorphism of amyloid fibrils can be divided into two classes, filament polymorphism and core polymorphism [13]. Filament polymorphism is the variation of how the proto-filaments interact laterally with each other in forming fibrils. Core polymorphism relates to the arrangement of monomers in the cross-β core. An important note is that the amyloid protein morphology can be highly dependent on the solution conditions found in vivo or used in vitro [17].

2.3 Thermodynamics - Equilibrium and solubility

Proteins have the possibility to form different folds, both intermediary folds as well as the fold with the lowest free energy, the most stable state. When a protein for a given system has reached this lowest free energy state, the system is referred to as having reached equilibrium. A system may not always reach equilibrium in short timescales and the system may only appear to have reached equilibrium, although it is instead in what is known as an apparent equilibrium. Kinetically trapped states may also be observed, where what prevents them from reaching true equilibrium are high energy barriers. A method for determining if a system has reached a true equilibrium is utilising the fact that a true equilibrium is reached independent on where along the pathway a reaction begins.

Solubility is generally defined as the concentration of a given molecule which can be dissolved in a solution without falling out. In the context of systems comprised of amyloid proteins it is often defined as the concentration of monomeric amyloid protein in solution, remaining un-aggregated. At true equilibrium, an initial system with 100% fibrils would dissolve and reach a monomer concentration at the solubility of the amyloid protein. Solubility for an amyloid protein can be described in terms of chemical potential. The chemical potential of a monomeric amyloid protein can be calculated according to equation (1), with R being the gas constant and T the temperature [1]. μ_m^0 is the standard chemical potential for α-synuclein and the activity of the monomer can be approximated as the concentration in a dilute solution [1]. The chemical potential can be defined as the partial derivative of Gibbs free

energy.

$$\mu_m = \mu_m^0 + RT \ln [m] \tag{1}$$

As a consequence of the second law of thermodynamics, a peptide will have the same chemical potential in every phase of a system independent on the number of phases of the peptide. Therefore, amyloid protein (or peptide) which are in fibrils, seen as a different phase will have the same chemical potential as those in monomeric form. The chemical potential of amyloid protein monomers in fibrils, μ_f equals the standard chemical potential, μ_f^0 if viewed as in a pure phase. This, due to the highly ordered structure makes the translational entropy term ($RT \ln[m]$) negligible [10]. In a system comprised of both monomers and fibrils, the solubility can be derived with equation (2) [1]. Also noted is how the solubility would be lower for a fibril with lower chemical potential. A more stable fibril morph would lead to a lower solubility [1].

$$[m] = \exp \frac{\mu_f^0 - \mu_m^0}{RT} \tag{2}$$

For a system comprised of 100% monomeric amyloid protein at a concentration above the solubility, aggregation will occur. Amyloid protein above solubility will form fibrils. If the monomer concentration was measured at equilibrium as a function of initial monomer concentration, one would expect a linear region with a slope of 1 below solubility. This region would then flatten out and stay at the solubility for all initial concentrations above solubility. If this measurement however was made at time 0, instead, the expected graph would be linear with a slope of 1 for all initial monomer concentrations, since of course no protein has aggregated. Due to the described lag phase of fibril aggregation, there is a phenomenon occurring between initial measurements and true equilibrium known as a "metastable region" [1]. This region, seen in figure 4, is time dependent and decreases with time. As the higher initial concentration systems will fibrillate faster, they will reach equilibrium first and the concentrations just above solubility will take the longest, leading to the triangular shaped metastable region.

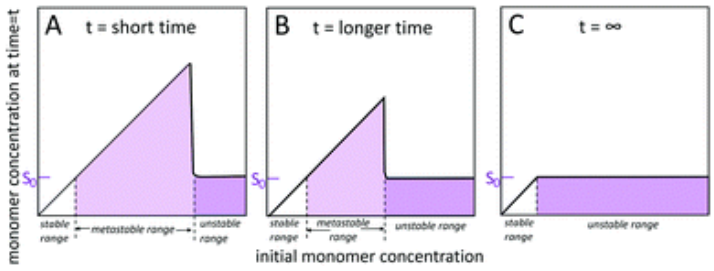

Figure 4: Illustration of metastable region in amyloid protein aggregation. [18]

2.4 α-synuclein

α-synuclein is a 14 kDa, 140-amino acid long protein found mostly in the brain, in particular the neocortex, hippocampus, substantia nigra, thalamus and cerebellum [19] [7]. Typically, α-synuclein is referenced in relation to its importance in Parkinson's disease and Lewy-body dementia. α-synuclein is known to aggregate and form inclusion bodies know as Lewy bodies in neurons of patients with these diseases. The function of α-synuclein has not been fully determined, but a study by Burr et al. (2010) describes α-synuclein as important in the formation of the SNARE-complexes involved in synapses [20]. The release of neurotransmitters is fundamental in synaptic activity, these neurotransmitters are released as vesicles and undergo fusion with the presynaptic membrane. This fusion requires SNARE-complex formation and Burr et al. (2010) showed a promotion in SNARE complex formation when bound to α-synuclein [20].

Structurally, α-synuclein only has a defined fold when bound to membranes, seen in figure 5. Its structure can be divided into three domains, an N-terminal membrane binding alpha-helical domain (residues 1-60), the non-amyloid-β-component (NAC) domain (residues 61-95) and an acidic C-terminal (residues 96-140) [7] [21]. Examining the amino acid sequence of the N-terminus region, it has a highly conserved KTKEGV hexameric motif, repeated every 11 amino acids. The ability to bind membranes and fold to form a defined structure is related to these motifs [7]. The NAC domain is the cause for fibril formation, and is where the cross-β core structure typical in amyloid fibrils is formed [7] [22]. The C-terminus is in a random coil conformation, believed to be caused by the high net negative charge and low hydrophobicity preventing interactions and formation of an ordered structure. Interactions between the NAC domain and the C-terminus is thought to prevent α-synuclein aggregation. By lowering of pH in solution, the net negative charges have been shown to be neutralized, promoting aggregation of α-synuclein [7].

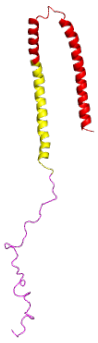

Figure 5: α-synuclein structure bound to an SDS micelle. Red is the N-terminal domain, yellow is the NAC region and magenta is the random coil C-terminal region. Retrieved from PDB file 1XQ8.

2.5 Chaperones

Due to the risk of protein spontaneously misfolding, the human body has employed a family of proteins known as chaperones to prevent this. These proteins can be defined as "any protein that interacts with, stabilizes or helps another protein to acquire its functionally active conformation, without being present in its final structure" [8]. Originally, the idea of chaperones was that they played an important role in the formation of proteins. However, with time, they have been shown to also be important all throughout the lifetime of proteins. Intrinsically disordered proteins, are some such proteins which are highly dependent on chaperones, as they, under normal conditions, are found unfolded.

2.5.1 DNA-JB6

Hsp70 (heat shock proteins 70) is a family of chaperone proteins which are expressed as a response to stress. They have several different functions such as helping in folding of nascent proteins as well as reversing misfolding of proteins. This is made possible through the use of an allosteric ATP hydrolyzing substrate binding cycle, allowing for binding to substrate proteins in need of the Hsp70 machinery [23]. As a help to this family of proteins are other classes of chaperones, one of which is the Hsp40 family. Also known as the DNAJ-protein family, they are identified by their highly conserved J-domain. The protein family is divided into three classes, DNAJA, DNAJB and DNAJC. Their differences lie in their structural composition. DNAJA has a N-terminal J-domain, a glycine and phenylalanine rich region, a zinc finger region and a beta-sheet heavy C-terminal domain involved in substrate binding.

DNAJB proteins have the same structure as DNAJA proteins, except for having no zinc finger region. DNAJC proteins only share the J-domain with the other classes [23] [24]. The J-domain consists of four helices, helices 2 and 3, together with a connecting loop, containing the HPD motif, interacts with Hsp70 proteins. The allosteric binding of ATP is promoted by the interaction with the J-domain of Hsp40 proteins. DNAJB6 is a 27 kDa protein from the DNAJ-protein family, in the DNAJB class. See figure 6 for general regions in DNAJB proteins. This protein has been shown to prevent aggregation of amyloid fibrils without the need of the Hsp70 proteins. However, it has also been shown that a highly conserved serine and threonine rich region in DNAJB6 is necessary for the ability to reduce and delay aggregation [25] [26] [27].

Figure 6: Illustration of DNAJB protein regions consisting of a J-domain N-terminal, a glycine/phenylalanine rich region and a beta-sheet heavy C-terminal.

2.5.2 The unhappy chaperone

The paper by Linse et al. (2021) introduces the "unhappy chaperone" hypothesis as a thermodynamic explanation about how chaperones prevent misfolding and aggregation of proteins [10]. Chaperones have been shown to increase the solubility of amyloid proteins. This is believed to be caused by the amyloid protein monomers forming co-aggregates with chaperone monomers.

As previously explained, the chemical potential of a protein is the same independent on the phase. In a system with both amyloid protein and chaperones, for amyloid protein not interacting with chaperones, the chemical potential can be expressed according to equation (3). m_* is the monomer protein concentration in solution in a system with chaperones. The standard chemical potential, μ_m^0 is the same as in a system without chaperones as seen in equation (1), as it is an inherent property of the peptide or protein.

$$\mu_{m*} = \mu_m^0 + RT \ln [m_*] \tag{3}$$

If then protein monomers form co-aggregates, as with aggregates formed between monomers making fibrils, the standard chemical potential, μ_a^0 equals the chemical potential μ_a. Continuing along the premises already established, the secondary law of thermodynamics implies that at equilibrium, the chemical potential of monomers alone should equal that of monomers in co-aggregates. This together with equation (3) leads to equation (4).

$$[m*] = \exp \frac{\mu_c^0 - \mu_m^0}{RT} \tag{4}$$

With the assumption that chaperones increases the solubility of amyloid proteins, $[m_*] > [m]$, this means $\mu_a^0 > \mu_f^0$. The standard chemical potential of co-aggregates of monomers of a different structure than those forming fibrils must be higher for there to be an increase in solubility. This leads to the idea of monomers creating co-aggregates with chaperones, as has been demonstrated in other studies [9]. However, an increase in chemical potential for monomers in co-aggregates with chaperones would be unfavorable. A possible explanation for this would be if the chaperones themselves would decrease their chemical potential when forming co-aggregates. Illustrated in figure 7, is how a decrease in chemical potential for chaperones when in co-aggregates, if larger than the increase for amyloid protein, gives an overall decrease for the system. The requirement is that at equilibrium, the increase in solubility should be the same independent on the pathway. Starting from a system with fibrils or only monomers, the formation of co-aggregates with chaperones would lead to the same solubility.

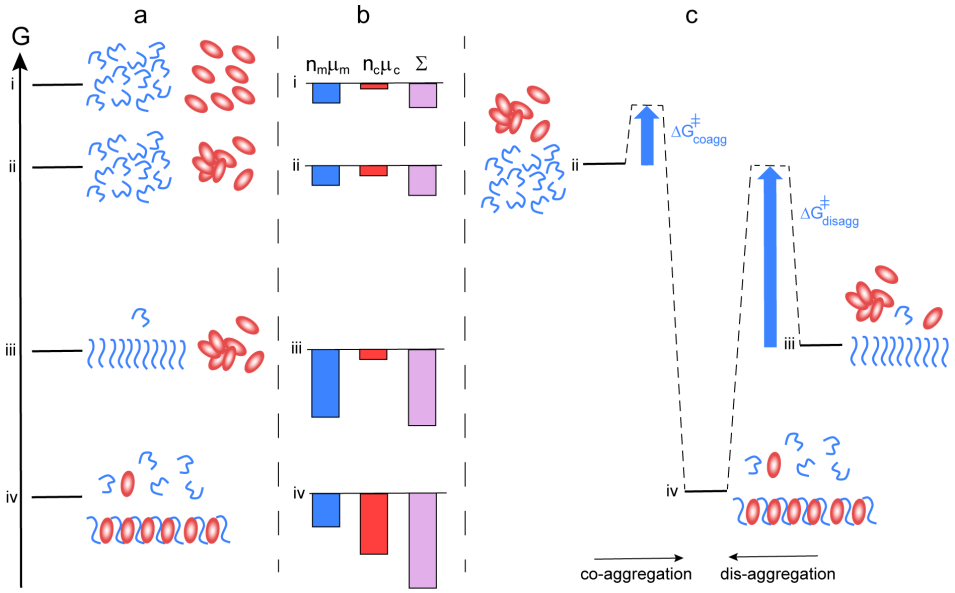

Figure 7: Illustration of chemical potential for amyloid protein and chaperone system. Blue is the total chemical potential for all amyloid protein in the system, red is the total chemical potential for all chaperones in the system and purple is the total chemical potential, i.e. the free energy of the system. System i contains only monomeric amyloid protein and chaperones, system ii is made up of monomeric amyloid protein and aggregated chaperones. System iii contains aggregated amyloid protein and aggregated chaperones with system iv containing co-aggregates of amyloid protein and chaperones. [10]

3 Materials and methods

3.1 Materials

- Wild type α-synuclein, already expressed and purified, was further purified in a 10 mM MES with 0.02% NaN_3, pH 5.5 buffer using an FPLC (Fast protein liquid chromatography), with a superdex 75 increase 10/300 Gl column.
- α-synuclein seeds were made by incubating 20 μM monomeric wild type α-synuclein over 3 days at 37° C with a magnetic stirrer. It was kept in pH 5.5, 10 mM MES buffer.
- Wild type DNAJB6 was already expressed and purified in 20 mM NaP buffer with 0.02% NaN_3 and 0.2 mm EDTA at pH 8.0. Buffer change to MES, pH 5.5 was then performed using FPLC.
- o-Phthaldialdehyde (OPA) reagent was used in protein concentration determination.
- Acetonitrile (ACN) with 0.1% trifluoracetic acid (TFA) was used as the mobile phase in HPLC protein concentration determination.
- Deuterium (D_2O) and 15N-tryptophan (standard) was added to all samples measured with NMR.
- Low binding tubes (Eppendorf Protein LoBind) or low binding 96 well plates (Corning 3881) were used for all sample handling or measurement.

3.2 Methods

The aim of the project was to measure the effect of DNAJB6 on α-synuclein aggregation and dis-aggregation. This required measurement of the solubility i.e. the monomer concentration. Part of this project was methods development to measure the monomer concentration reliably, the results of these developments and the eventual protocols will be presented in this methods section.

To measure the solubility, two main methods were determined to be used after weighing the pros and cons of several possible methods. The two methods of choice are OPA fluorescence and HPLC absorbance measurements. At all time points monomer concentration was measured, both methods were used simultaneously. As a third method, NMR was used to get alternative independent values on the solubility.

3.2.1 Experimental design

Firstly, monomer isolation of α-synuclein was done. Expressed and purified α-synuclein was frozen at -80° C and then lyophilized to increase yield after FPLC purification. Before injection into the FPLC, 1 ml guanidinium hydrochloride was used to dissolve the lyophilized protein and to denature it into monomeric form. A superdex 75 increase 10/300 Gl size exclusion column was used, to isolate the monomers. Monomeric α-synuclein was then extracted as the eluate and put on ice to be stored in a cold room to prevent aggregation. To determine the concentration of the eluate, the absorbance measured by the UV detector at 280 nm from the FPLC was averaged for the eluate volume. Through the Beer-Lambert law, $A = \epsilon cl$, the concentration, c was calculated with the molar absorptivity (ϵ) for α-synuclein, determined to be 5960 $M^{-1}cm^{-1}$. The length, l is 0.3 cm for the specific FPLC and A is the absorbance.

After purification of monomeric α-synuclein, the main experiments could begin. The experimental design to follow the aggregation and dis-aggregation of α-synuclein is seen in figure 8. The experiment can be divided into four groups, two of which follow the aggregation, one without DNAJB6 and one with 0.98% DNAJB6, rounded to 1% for the rest of the report. The purpose of following aggregation without DNAJB6 was to determine a solubility of α-synuclein, specific for the conditions in this project,

to compare with samples with DNAJB6. The other two groups follow dis-aggregation. After letting α-synuclein aggregate, DNAJB6 was added at two different concentrations. The dis-aggregation was measured by diluting a stock solution of aggregated α-synuclein down to the desired total α-synuclein concentrations (2.5, 5, 10, 20 μM). The dilutions were done with the addition of the DNAJB6 at concentrations relative to α-synuclein of 1 and 10%, these values are rounded to 1% and 10% respectively for the rest of the report. 1% was chosen to compare with the forward aggregation at the same concentration, whereas 10% DNAJB6 was used to get a stronger effect. When extracting samples for measurement, 100 μl was pipetted up from the incubation tubes and transferred to smaller tubes. These were then centrifuged at 31510 RCF (18000 RPM) for at least 30 minutes but most times, 60 minutes or more.

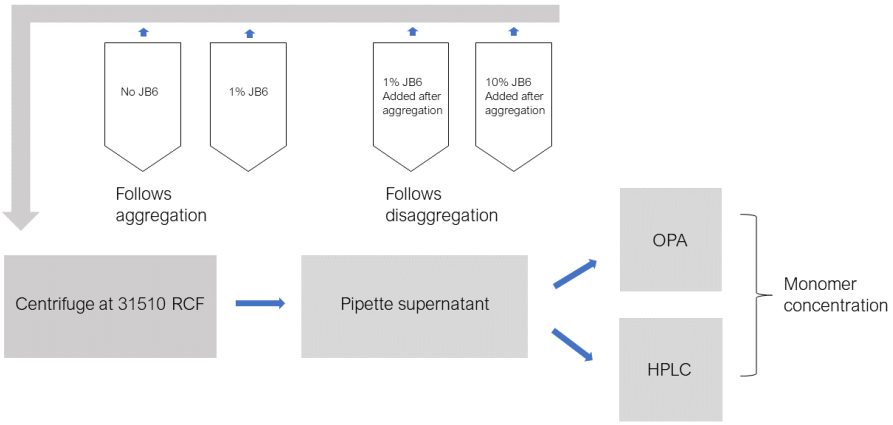

Figure 8: Workflow of measuring monomeric α-synuclein with OPA fluorescence and HPLC absorbance.

The incubation conditions for the aggregation of α-synuclein are as following. 37° C and 2% seeds were necessary to initiate aggregation under acceptable timescales since the samples were kept in low binding tubes. pH 5.5 was chosen as due to it being where secondary nucleation of α-synuclein is the most prominent [28]. Tubes were kept at 100 rpm to prevent sedimentation of aggregates and allow α-synuclein and DNAJB6 to interact without perturbing the system too much. 0.2% NaN_3 was also added to prevent growth of any bacteria. Instead of using replicates, the experiments were done at 4 different total α-synuclein concentrations, 20, 10, 5 and 2.5 μM. This is because the solubility, if below these initial concentration should be reached by them all if at true equilibrium.

3.2.2 OPA

o-Phthaldialdehyde (OPA) is a reagent used for protein concentration determination (figure 9). As a reagent it binds to all primary amines i.e. all protein, but could also react with contaminants. Of note is that DNAJB6 have 28 lysines which are primary amines, and α-synuclein have 15. Advantages of using this specific reagent are that it is ease of use, it is affordable and reproducible. If each measurement is done with a standard it is also quite robust. OPA when reacting with protein excites at 340 nm and emits light at 455 nm [29]. The protocol used for OPA fluorescence was already developed.

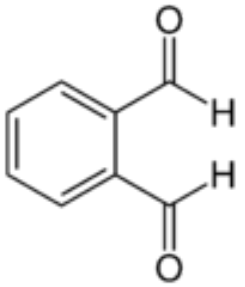

Figure 9: Chemical structure of o-Phthaldialdehyde.

Supernatant from centrifuged samples containing only non-fibrillar α-synuclein species and possibly DNAJB6, is extracted. 25 μl per sample is mixed with 25 μl OPA, to then be measured with a CLARIOstar microplate reader. Each plate measurement was made with a standard of 8 concentrations and 3 replicates, see appendix A1 for standard curve example.

3.2.3 HPLC

The HPLC (high-performance liquid chromatography) uses absorbance to measure protein concentration at 214 and 280 nm. This specific system uses a BIOshell™ A160 Peptide CN, 2.7 µm column, based on reversed-phase chromatography. Reversed-phase elutes depending on the hydrophobicity of the sample. More hydrophobic protein or peptide would bind harder to the column and elute later than less hydrophobic ones.

After testing of several different protocols, a final protocol which aims to give the highest sensitivity for α-synuclein signal was developed. Important parameters for the protocol are the flow rate set at 2 ml/min, column oven temperature set at 40° C and the use of 50 μl sample. The gradient used is seen in figure 10. At sample injection, the mobile phase is at 100% water, this is believed to lead to all of the protein in the sample adsorbing onto the column highly concentrated due the highly unfavorable polar environment, leading to higher sensitivity. Next, the mobile phase increases to 30% ACN in a gradient. After testing, this was determined to be the sufficient percentage of organic solvent to elute α-synuclein and was the most optimal in comparison to using a step gradient or an isocratic elution. After the protein has left the stationary phase, a gradient is used to reach the cleaning stage at 80% ACN, which cleans for 2 minutes (8 column volumes). Finally, the column is re-equilibrated to 100% water.

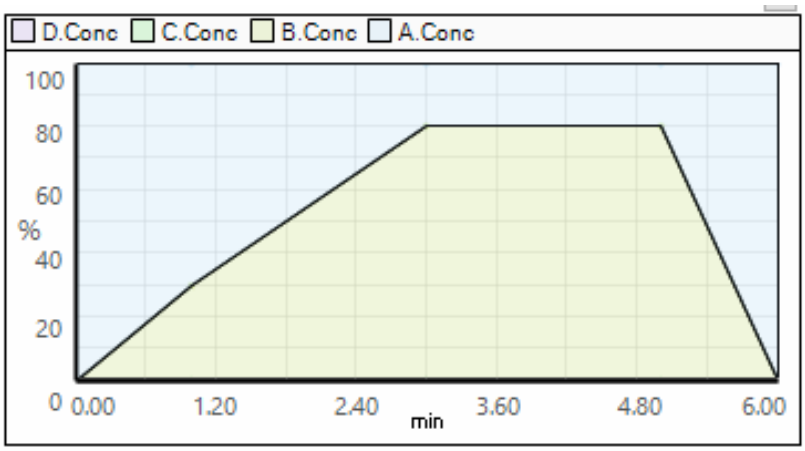

Figure 10: Gradient used for α-synuclein protein concentration determination in HPLC.

A typical chromatogram for a α-synuclein sample can be seen in figure 11a. Elution is at around 1.56 minutes which can be compared to the elution of DNAJB6 which is at around 1.80 minutes, see figure 11b.

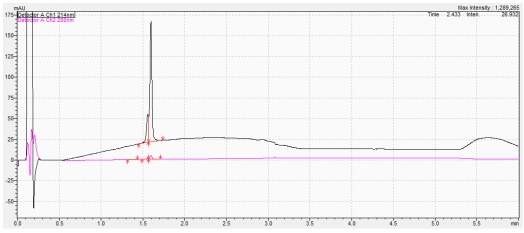

(a) Chromatogram for alpha synuclein concentration determination.

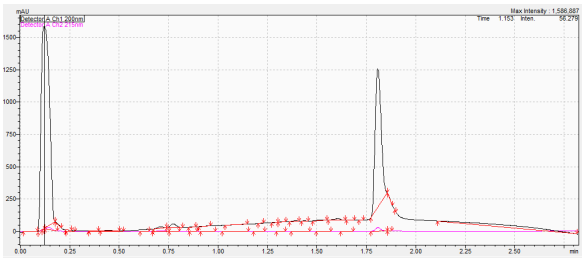

(b) Chromatogram for DNAJB6 elution.

Figure 11: HPLC absorbance chromatogram for elution of α-synuclein and DNAJB6 at 214 and 280 nm.

3.2.4 NMR

Nuclear magnetic resonance or NMR is a technique utilizing the phenomenon of molecular nuclei resonating at different frequencies when applying a magnetic field. This allows for highly detailed structure determination of molecules. There are several different methods when using NMR, depending on what the purpose of the study is. For the purpose of concentration determination and achieving the highest possible sensitivity as well as molecular distinction, 2D HSQC with 15N labeled protein was used. In these experiments, each nitrogen and amide hydrogen, in each residue of a protein will give a signal in the recorded spectra. The results is a 2D spectra with "fingerprint" like signal peaks, specific to the given protein.

In the case of α-synuclein, the fibrils are too large to be detected by the NMR. Therefore, only the monomers will give a signal and the intensity can be followed as a function of time to measure the solubility of α-synuclein. As a means to get an absolute value of the concentration of monomeric α-synuclein, a 2.5 μM standard was added to the measured sample. In figure 12, a recorded 2D HSQC spectrum for α-synuclein can be seen at initial measurement and after 3 days. Each spectrum was recorded for 1.5 h, so for 3 days around 48 spectra were made. The decrease in intensity is clearly

visible. When measuring the intensity, through the tools in the software (TopSpin), the integral of a chosen peak could be calculated.

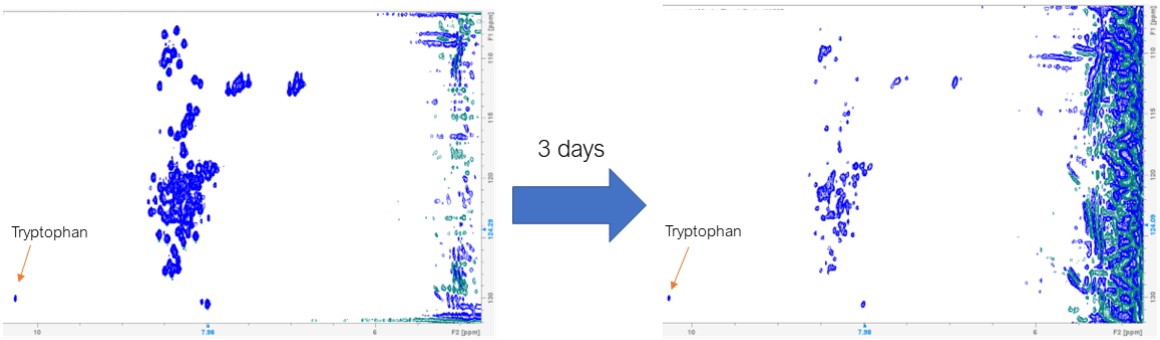

Figure 12: 2D HSQC spectra for 15N labeled α-synuclein with tryptophan standard.

The experiment was setup with an initial concentration of 20 μM total α-synuclein, 2% seeds, 10% of the total volume of D_2O to suppress the water signal and 2.5 μM tryptophan. Next, the sample was measured for 3 days in the NMR at 37° C, to then be incubated at the same temperature for 2 weeks. Then the sample was again measured for 24 hours to get a new value for the solubility. 10 % DNAJB6 was then added to the sample and measured for 3 days, again the sample was incubated for 2 weeks at 37° C to then be measured on for 3 days a means to measure possible disaggregation of the fibrils.

3.2.5 SDS-PAGE/MALDI

Two additional methods were used to determine the contents of the samples. The first method is SDS-PAGE, which is a method based on electrophoresis, allowing for separation of proteins by their mass. SDS (sodium dodecyl sulfate) breaks intermolecular interactions in proteins, effectively breaking them down into their monomeric form. As a micelle, SDS has a polar head and a hydrophobic tail. These regions interact with the corresponding regions of the target protein. Furthermore, SDS is comprised of negative charges, which for most proteins will result in the protein being straightened out by the charges. The negative charges of the SDS are proportional to the mass of the protein. Since the ratio of charge to mass is the same for most protein after SDS addition, when applying a voltage over a gel, loaded with the proteins mixed with SDS, they will be ordered by their mass while traveling with their charge. This is illustrated in figure 13. In the analyzed samples, 15 μl was mixed with 15 μl Novex Tris-Glycine SDS loading dye and boiled for 3 minutes before running the gel at 120 V for 60 minutes. As a standard, PageRuler prestained protein ladder was used.

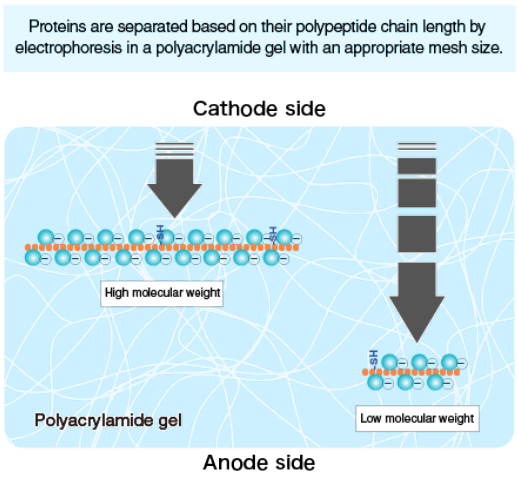

Figure 13: Illustration of protein travelling on SDS-PAGE gel. [30]

The second method was MALDI (matrix-assisted laser desorption/ionization) mass spectrometry. This method is based on "shooting" your sample with a laser which ionizes the sample, giving it charges that can travel along a vacuum that has an applied electric field over it. As the ions travel towards a detector, the time-of-flight is recorded for each ion. Since the time is related to the mass over charge ratio of the ion, each recorded ion can be characterized. Smaller molecules would travel faster than larger molecules.

4 Results

4.1 Solubility of α-synuclein

As a first experiment, there was a need to determine the solubility of α-synuclein in the environment chosen. Seen in figure 14 is the measured monomer concentration at different time points (all graphs in the results section have been produced with GraphPad Prism 9 software). After 120 h, a first apparent equilibrium is reached. With time however, the monomer concentration decreases and reaches new apparent equilibrium. At the final measured apparent equilibrium after 837 h, the solubility is determined to be 0.39 ±0.016 μM with OPA and 0.11 ±0.013 μM with HPLC. The lack of linearity for the initial measurements with HPLC, is thought to be attributed to faulty runs specific to the HPLC. Since each sample measured in the OPA and HPLC is taken from the same tube after centrifuging, the results from the OPA indicates errors in the HPLC. Important to note is the decrease in apparent solubility with time seems to decrease. In fact, when measured with OPA between 331 h and 837, the value even increases slightly from 0.36 μM to 0.39 μM, indicating that it has reached apparent equilibrium not attributed to the faster aggregation for high initial concentration of α-synuclein.

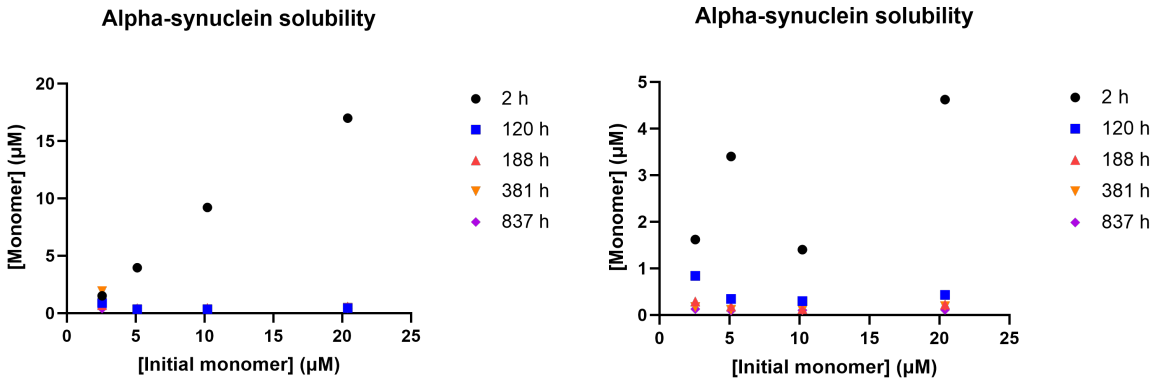

(a) Measured with OPA.

(b) Measured with HPLC.

Figure 14: Monomer concentration against initial monomer concentration at different time points for α-synuclein aggregation at pH 5.5. After 120 h, a first apparent equilibrium has been reached.

4.2 Effect on aggregation in presence of DNAJB6

Next, the effect of DNAJB6 on the aggregation of α-synuclein was measured. Seen in figure 15 is how an apparent equilibrium is reached after 188 h when measured with OPA and after 120 h with the HPLC. After 120 h, when measured with OPA, the aforementioned metastable region is visible with the higher initial concentration α-synuclein samples aggregate faster. As without DNAJB6, the apparent solubility decreases with time, but contrary to the measurements without DNAJB6, at 837 h there is larger decreases in the apparent solubility between time points. this indicates that the system has not reached an apparent equilibrium which could be regarded as the solubility of the system.

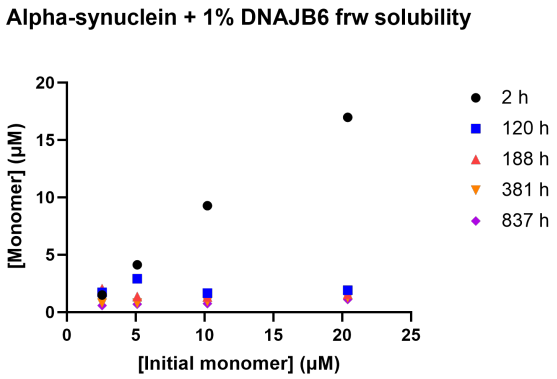

(a) Measured with OPA.

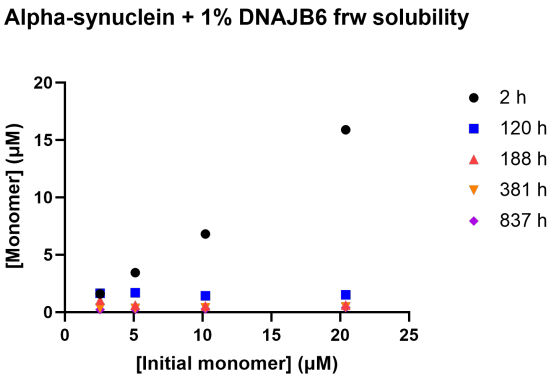

(b) Measured with HPLC.

Figure 15: Monomer concentration against initial monomer concentration at different time points for α-synuclein aggregation at pH 5.5 with 1% DNAJB6. After 120 h, a first apparent equilibrium has been reached.

To compare the aggregation of α-synuclein w/wo DNAJB6, using the different initial concentrations as "replicates", the monomer concentration was plotted against time, seen in figure 16. These graphs show all time points except for initial measurements as it is shown to illustrate the solubility and apparent equilibrium. Visible is the higher monomer concentration in samples with the addition of DNAJB6. A clear indication is that DNAJB6 seems to delay the aggregation of α-synuclein. Whether or not the DNAJB6 increases the solubility can not with certainty be concluded. Although the decrease in monomer concentration may seem to have reached a plateau, if it is only a delay or a true apparent equilibrium is not easily determined with these time points.

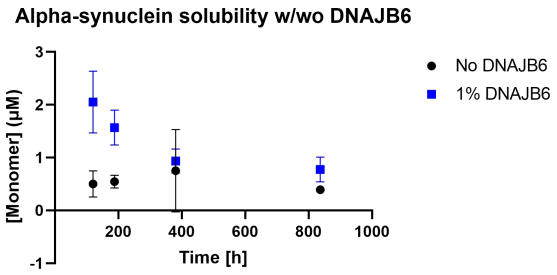

(a) Measured with OPA.

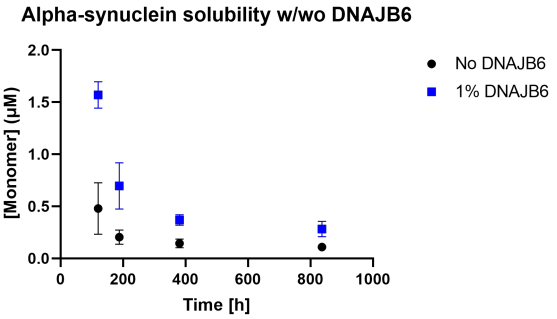

(b) Measured with HPLC.

Figure 16: Monomer concentration against time for α-synuclein aggregation at pH 5.5 w/wo 1% DNAJB6.

4.3 Effect on dis-aggregation in presence of DNAJB6

The addition of DNAJB6 to the dis-aggregation samples were added to a stock solution of fibrillar α-synuclein, total α-synuclein concentration was diluted down by the DNAJB6, and so was the monomer concentrations. Therefore, as seen in figure 17, at initial measurements the monomer concentrations are linear. However, the expectation is that the monomer concentrations would increase since they have been diluted below solubility, to reach apparent equilibrium. They should also all reach the same

monomer concentrations and thereby plateau. The opposite is seen with the monomer concentrations decreasing, as if above solubility. Interesting is that for the final time point, at 837 h, the monomer concentrations seem to stay the same when measuring with OPA and even slightly increasing for the higher total α-synuclein concentrations with HPLC. Important to note, figure 17a is without an outlier, see appendix A2 for graph with outlier.

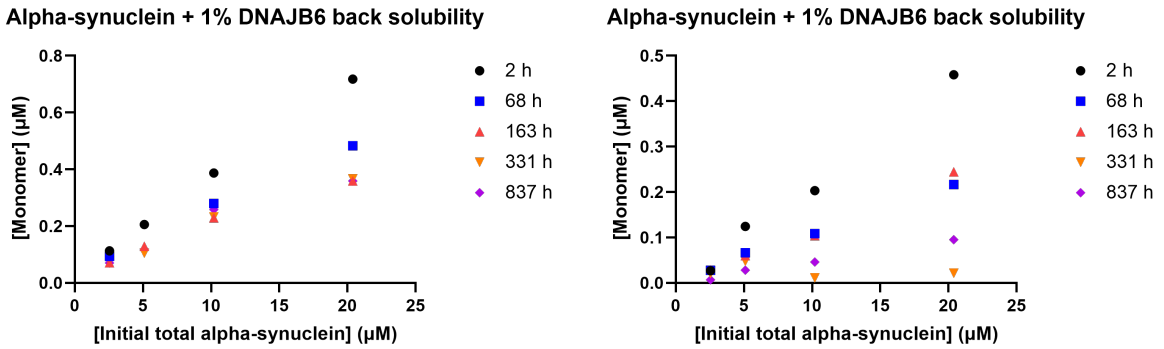

(a) Measured with OPA.

(b) Measured with HPLC.

Figure 17: Monomer concentration against initial total α-synuclein concentration at different time points for α-synuclein dis-aggregation at pH 5.5 with 1% DNAJB6. An outlier at 68 h, with initial concentration of 5 μM was removed.

The addition of 10% DNAJB6 gives similar results as for 1% DNAJB6. The decrease in monomer concentration is seen both with OPA and HPLC, see figure 18, however only the measurements with OPA see an increase at the final time point.

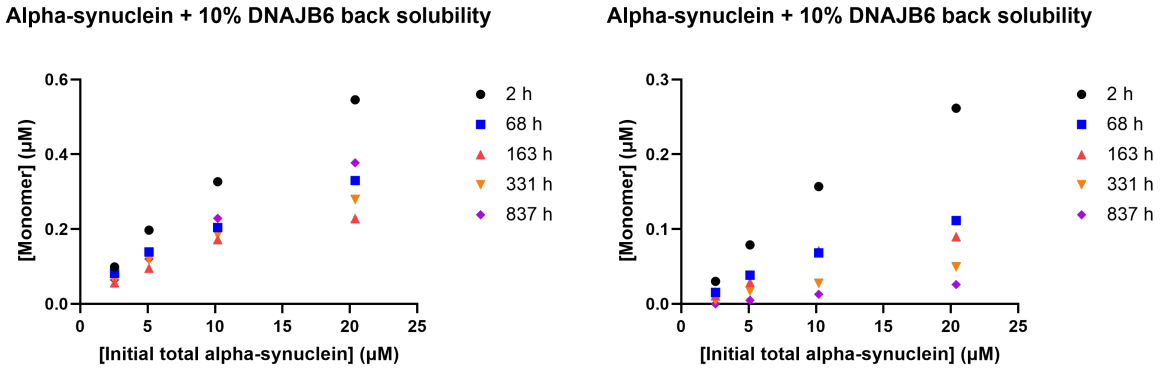

(a) Measured with OPA.

(b) Measured with HPLC.

Figure 18: Monomer concentration against initial monomer concentration at different time points for α-synuclein dis-aggregation at pH 5.5 with 10% DNAJB6.

The aggregation of α-synuclein with 1% DNAJB6 gave rise to an unexpected gel-like compound seen in figure 19. It is only clearly visible when pipetting in the tube as it otherwise is placed at the bottom. The image was taken as the compound was floating in the tube. To further analyze the constituents of the compound, mass spectrometry was employed.

Figure 19: Sample with α-synuclein + 1% DNAJB, following aggregation. Marked in the image is the formation of a gel-like compound.

Through the use of a MALDI (matrix-assisted laser desorption/ionization) mass spectrometer, the gel-like compound in figure 19 was analyzed to determine its constituents. When retrieving the compound for analyzing, it fragmented into more cloudy like aggregates, seen in the samples of α-synuclein aggregation without DNAJB6. To dissolve the compound/aggregates, acetonitrile and TFA was used. The results are seen in figure 20. Peaks for α-synuclein monomer, dimer and DNAJB6 monomer was identified. This could indicate the formation of aggregates containing α-synuclein and DNAJB6.

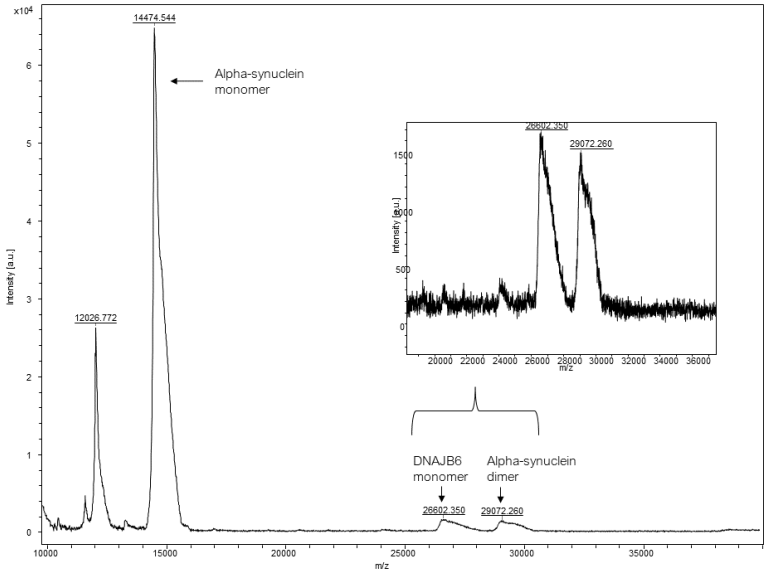

Figure 20: MALDI spectra on α-synuclein + 1% DNAJB6 aggregation sample. Identified is a α-synuclein monomer and dimer peak, and a DNAJB6 monomer peak.

4.4 SDS-PAGE analysis on protein

To determine the constituents in the different reactions, two SDS-PAGE gels were run. The first one was done on non-filtered samples after 15 days, which is seen in figure 21. As expected, α-synuclein is found for all samples, those with a higher concentration of total α-synuclein gave more intense bands (20 μM > 10 μM). Regarding the DNAJB6 bands, those were found in the samples with DNAJB6, and had a higher intensity for the samples with 10% DNAJB6 than for those with 1% DNAJB6. Interesting is that the DNAJB6 bands for the dis-aggregation are more visible than for those in the forward aggregation. Unexpectedly, there are also several other bands appearing, less intense for the forward aggregation reaction, yet still identifiable. One of these bands, just above the DNAJB6 bands, is at the position corresponding to the molecular weight of dimeric α-synuclein.

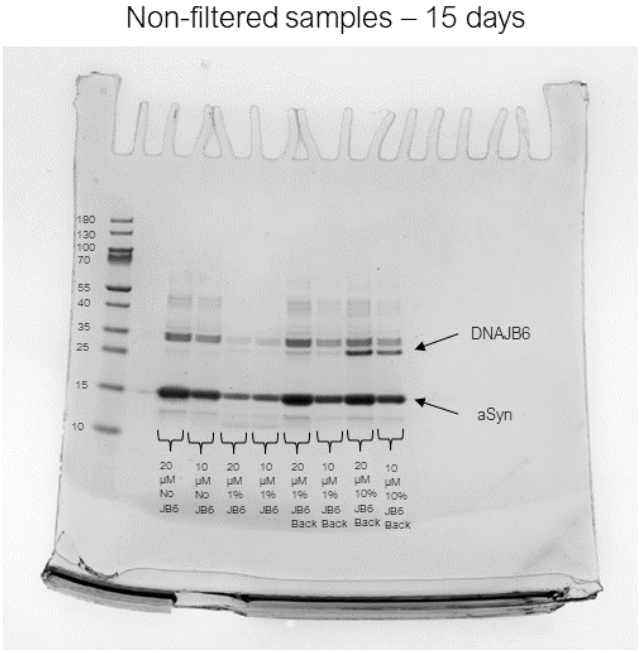

Figure 21: SDS-page analysis of non-filtered α-synuclein + DNAJB6 samples after 15 days. Molecular weights for ladder are in kDa.

The second gel run was on filtered samples after 20 days, using AcroPrep 96 well filter plates, see figure 22. Since the filters are expected to remove all aggregates, only monomeric α-synuclein and DNAJB6 should be in the samples used in the gel. α-synuclein is identified, but no DNAJB6 bands are visible. Either the monomeric DNAJB6 did not go through the filters, or they have all formed aggregates which also would not go through the filters.

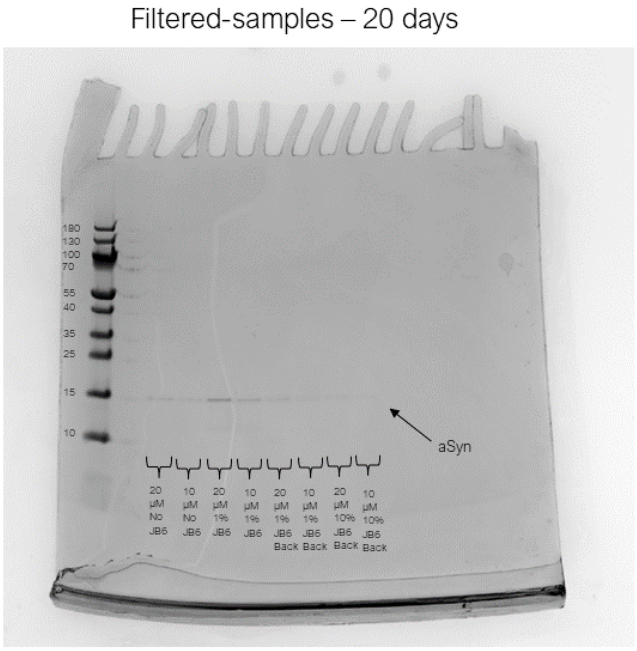

Figure 22: SDS-page analysis of filtered α-synuclein + DNAJB6 samples after 20 days. Molecular weights for ladder are in kDa.

4.5 NMR spectroscopy to follow dis-aggregation in presence of DNAJB6

First, there was a need to determine the viability of measuring α-synuclein monomer concentration while also not detecting fibrils. Simply inspecting the fingerprint spectra at the initial measurement and the final time point as done in figure 12, there is a clear reduction in monomer concentration. If it only detects monomers can not be concluded from this. However when plotting the monomer concentration as a function of time, seen in figure 23, the existence of a lag-phase, a exponential region and a plateau would indicate monomer concentration is only detected. The apparent solubility can be estimated as the average monomer concentration for the final 8 measurements as 2.56 $\pm$0.43 μM.

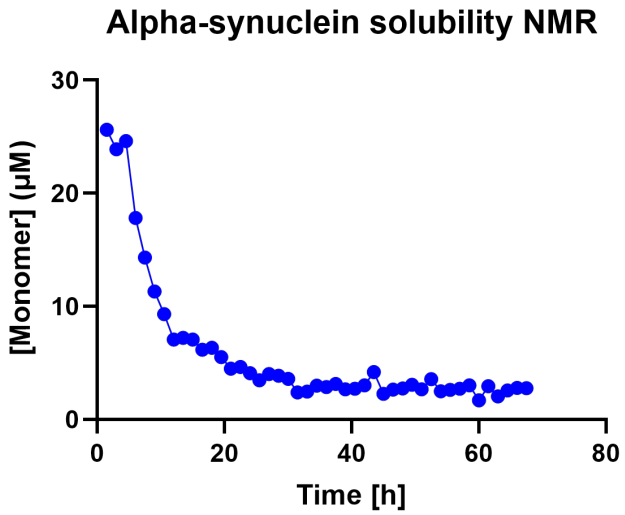

Figure 23: α-synuclein solubility measured with NMR.

Next, the same sample, kept in the same NMR tube was put in a 37° C incubator for 2 weeks. After those 2 weeks the tube was put in the NMR spectrometer and measured on for 24 hours to get a new value for solubility. This is seen as the blue points in figure 24, the average value for those data points is 6.83 ±0.90 μM. 10 % DNAJB6 was then added to same sample, this was then measured for 3 days, seen as the green data points in figure 24. The decrease in monomer concentration can partly be explained by the dilution of α-synuclein by the addition of DNAJB6. The average monomer concentration for the first 3 data points after addition of DNAJB6 is 3.64 ±0.08 μM. There is a slight trend upwards during the 3 days of measurement. Finally, the sample was incubated again for 2 weeks, to then be measured again for 3 days, seen as the black data points in figure 24. The average monomer concentration for those is 5.88 ±0.37 μM.

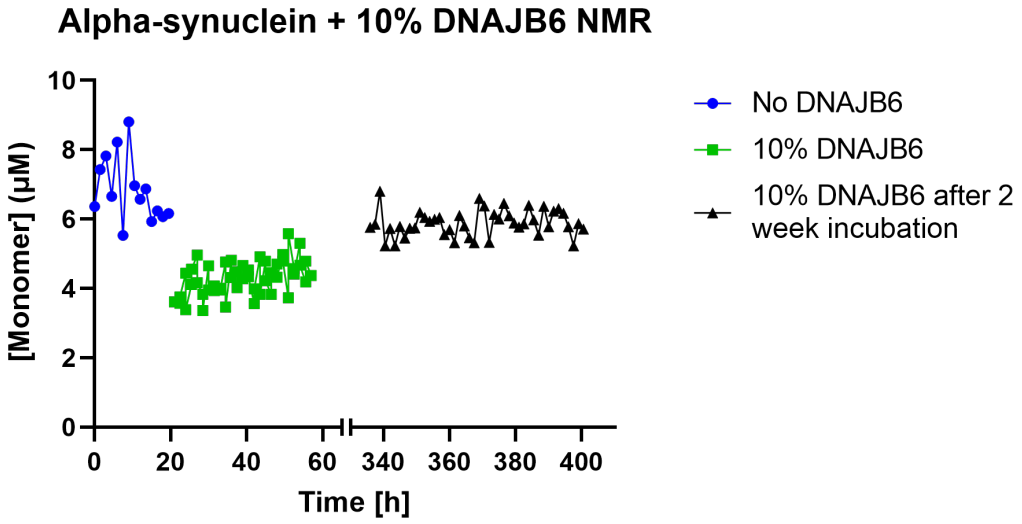

Figure 24: α-synuclein solubility + DNAJB6 measured with NMR.

5 Discussion

It is first important to mention that the determination of an absolute value of the solubility of α-synuclein for all systems is not possible. The aggregation and thereby the solubility of α-synuclein and other amyloid protein is dependent on the environment in which the aggregation occurs, but also where the measurement takes place. Variations in temperature, pH, salt concentration and other factors all contribute to the determined solubility for the given system. As previously mentioned, the morphology of the fibrils is dependent on the conditions used to generate it in vitro. With different morphologies, the systems would be different and therefore the solubility could be as well.

5.1 Measuring of α-synuclein solubility

Solubility, as described, is the concentration of monomers in the system at equilibrium. Since the amounts of total monomeric α-synuclein should not play a part in the equilibrium state of the system, only on the kinetics, the choice to use multiple different initial concentrations of monomer was chosen over using replicates. Optimally, both would be done, however, each sample require much preparation when initiating the reactions but also each time monomer concentration is measured. One issue when starting the experiments is wanting to start all experiments from the same purified batch, since the solubility depends not only on the conditions but also on the purification. However, when purifying the monomeric α-synuclein, if one would purify a large batch, there arises issues with whether the size-exclusion chromatography can produce monomeric α-synuclein or if there would be more oligomeric states produced as well.

Examining the initial concentrations of the α-synuclein monomer when measured with the HPLC, the values are not as expected. The linearity seen when measuring with OPA is expected here as well. When extracting samples for measuring after centrifuging, 25 μl for the OPA is taken first, before 60 μl is taken for the HPLC. The monomeric α-synuclein should be homogeneous all throughout the centrifuged tube and the fibrils should be centrifuged to the bottom. Therefore, if there was to be more α-synuclein in any of the two methods, it would be for the HPLC where fibrillar α-synuclein could possibly be pipetted with monomeric protein. The opposite is seen in the results, which leads to consideration of whether there are issues with the measurement. Because the measurements at other time points or for other samples do not give such strange readings, it would be more likely to be due to human errors in the handling of the samples. Other than that, there could be losses in the tubing or column of the HPLC. However, these should be accounted for, as there is a standard curve made from the same batch of α-synuclein. Since the initial measurement only should act as a confirmation of how much sample is in the different sample tubes, having issues specifically that time is acceptable. Especially since the OPA gives a confirmation on the actual values.

Another important consideration for the measurements is the temperature. While the samples are incubated at 37° C and the centrifugation also is done at the same temperature, there is downtime in between which might factor in. Extracting sample from the larger tubes where the reaction takes place, to the smaller tubes for centrifugation, moving the tubes to and from centrifuge, extracting sample for measurement into 96 well plates, adding OPA for fluorescence measurements and setting up the HPLC are all times where the system is not corresponding to the reported one. However, there are reasons why this may not be so significant. First, the aggregation of α-synuclein takes place over time-scales of at least 10 hours depending on the system. Therefore, even if the handling of samples would take up to 1 hour, it would not be enough time to disrupt the measurements significantly. The one time would be for the initial measurements, at the other time points, most of the time the system has reached apparent equilibrium and so the aggregation would be slow. Furthermore, the samples are kept in a cold compartment in the HPLC at 8° C until after the OPA measurements. At this temperature α-synuclein has very slow aggregation, almost at the point where cold denaturing would take place.

It is interesting to compare the determined values to literary values, although as mentioned, any values determined would be specific to the conditions. The α-synuclein critical aggregation concentration (CAC) as measured by Afitska et al. (2019) is 0.4 μM. Their conditions were, pH 7.2 with 6 mM $Na - PO_4$, 37° C, 140 mM NaCl, 10 mM NaN_3 and 1 mM EDTA [31]. CAC is the concentration at which aggregation occurs, and they measured it by following at what concentration there was no increase in ThT (thioflavin t) signal, which is an indicator of fibril mass. Unlike our experiments there is no direct measurement of monomer concentration, so while their value is not the solubility of α-synuclein, if the thought that solubility is the concentration above which fibrillation occurs, the CAC would effectively be the same as the solubility. The determined value for our study is 0.39 $\pm$0.016 μM or 0.11 $\pm$0.013 μM and as mentioned there is no need to compare to exact values between two different systems, however it is clear that they are in the same range.

5.2 Effect on aggregation in presence of DNAJB6

From the results in figure 16, there is a clear delay and possible reduction in the aggregation of α-synuclein in the presence of 1% DNAJB6. The reason for the hesitancy to describe the aggregation as reduced is due to the lack of a plateau, constant enough. There is still a decrease in monomer concentration after 837 h. To determine an apparent solubility, there must not be a plateau with no decrease, however the decrease should not be substantial. While the decrease is not substantial on the scale of total α-synuclein concentration, the decrease is still larger than the decrease for α-synuclein aggregation without DNAJB6 at their respective plateaus. Therefore, there is no clear indication that the monomer concentration with DNAJB6 could not possibly reach the same level as for without DNAJB6.

An important factor in the handling and effectiveness of DNAJB6 is what state it is most active. There have been discussions within the group at the department of biochemistry and structural biology at Lund University, on whether it is the monomeric or dimeric conformation of DNAJB6 that interacts with the amyloid protein. Preliminary data has found the concentration at which only monomeric DNAJB6 is in solution to be around 100 nM. If it is this conformation that interacts with α-synuclein, it would be important to let the system in which DNAJB6 is to be used, allow the DNAJB6 to reach equilibrium between the monomeric state and the other oligomeric state. Without having a certain value for how long this takes, to allow for the most optimal effectiveness of DNAJB6, before adding it to the α-synuclein, the DNAJB6 was diluted to 2x above the final concentration. This dilution was done several days before addition to the α-synuclein, so that when adding it, the DNAJB6 has reached equilibrium. The monomeric DNAJB6 concentration would then be diluted to 2x below the equilibrium concentration which would not be very much less than if it was directly diluted from a higher concentration. Another consideration was towards surface adsorption. DNAJB6 has been found, according to data acquired by the department (Carlsson. Andreas), to be highly adsorptive to surfaces. Tests done on different tubes found Eppendorf Protein LoBind tubes to be the most effective, also important was to fill up as much of the tubes as possible to increase the volume to surface ratio, and to prevent shaking or flipping of tube.

Examining the SDS-Page figures, there is as expected α-synuclein and DNAJB6 in the non-filtered forward aggregation samples. For the filtered-samples there is only α-synuclein and no DNAJB6. Either monomeric DNAJB6 can not pass through the filter, or the DNAJB6 has formed some sort of aggregate which can not pass through. With the expectation that monomeric DNAJB6 should pass through the filter, the thought of DNAJB6 forming aggregates would fit well with the unhappy chaperone hypothesis. If the aggregates formed are between α-synuclein and DNAJB6 that could explain the increase in solubility.

When visually inspecting the aggregation samples with DNAJB6 there seemed to be a gel like aggregate formed. In the aggregation samples without DNAJB6, there was visual aggregates formed, however without the formation of a gel-like compound. In an attempt to determine what was in the

gel-like compound, mass-spectrometry was run. When extracting the compound, it broke down into more commonly seen fibrillar constituents. These were extracted and analyzed, and it was determined to contain α-synuclein and DNAJB6.

An interesting question is if DNAJB6 form fibrils with monomeric α-synuclein, and thereby delaying the formation of fibrils. Over time however, the system would reach solubility as the fibrils are still formed, albeit at a slower rate. Another possibility is that DNAJB6 form aggregates with monomers from the fibrils, effectively breaking up the fibrils.

5.3 Effect on dis-aggregation in presence of DNAJB6

This is the part of the experiment with the most unexpected results. The monomer concentration decreases over time even after diluting fibrillated α-synuclein. However, the thought before these experiments was that the solubility of α-synuclein was higher than determined here, therefore the dilution of fibrillated α-synuclein monomer concentrations to below solubility was expected to be achieved if below around 1 μM. Since the determined values of solubility was at 0.39 $\pm$0.016 μM or 0.11 $\pm$0.013 μM depending on the method, the decrease in monomer concentration after dilution could be explained by this. It had not reached true equilibrium yet and even after dilution it keeps decrease to reach equilibrium and solubility. With the addition of 1% and 10% DNAJB6, if the solubility is expected to increase then the monomer concentration should increase to above at least those two values. In the HPLC measurements, the monomer concentrations reach really low values, at or even below the limit of detection for the standard curves used. This could be explained by the OPA measurements also measuring DNAJB6, giving higher values, however the higher values are also found when measuring solubility without DNAJB6.

What is seen in the measurements with the OPA at the initial monomer concentration of 20 μM is how the monomer concentration stops decreasing in the case of 1% DNAJB6 and even increases for 10% DNAJB6. Elongation of fibrils as a reaction always goes in both directions at equilibrium, monomers are added to the ends but also removed. If these reactions are very fast, then the time it takes for the reaction of DNAJB6 forming aggregates with monomers from the ends of the fibrils, could take time. This would then explain how it takes time for the DNAJB6 to have an effect on the dis-aggregation of α-synuclein. Another aspect is the accessibility of DNAJB6 to the fibrils in the sample tubes. Fibrils formed sediment towards the bottom of the tube, there they might not be able to react as easily with the monomeric DNAJB6. The hope would be that the DNAJB6 should be homogeneous throughout the sample and "find" the fibrils at the bottom. In an effort to combat this, the samples were kept under slow shaking at 100 rpm. There is a balance between disturbing the sample and allowing the constituents to reach each other, however at 100 rpm there is close to no visible mixing inside the tube, so the system could be considered undisturbed. Sedimentation is not prevented either and improvements on the storing and incubation of samples are considered of great importance.

DNAJB6 forming aggregates with monomers not in fibrils could also explain the decrease in monomer concentration. Aggregates with free monomers would lead to less monomers at first, however over time, equilibrium would require the fibrils to dissolve and the monomer concentration increasing towards the true equilibrium. As with the forward aggregation reaction, the SDS-PAGE of the dis-aggregation show no DNAJB6 in the filtered samples. Again, contributing to the idea of aggregates formed between DNAJB6 and monomeric α-synuclein.

5.4 NMR spectroscopy

Before these experiments, it was not certain whether it would be possible to follow α-synuclein monomer concentration for the given system conditions. While it still is not certain if it is only monomeric α-

synuclein that is detected, the shape of the graph (see figure 23), plotted from the intensity of the 2D spectrum, is as expected when following aggregation of α-synuclein. The measured apparent solubility of 2.56 ±0.43 μM after 3 days, could be compared to the apparent solubility of α-synuclein after 5 days (120 h), which is 0.50 ±0.22 μM, with OPA and 0.48 ±0.21 μM, with HPLC. As previously mentioned, the morphology and thereby aggregation of an amyloid protein is dependent on the solution conditions. There are three main differences which could lead to the difference in solubility. Firstly, the α-synuclein is 15N labeled, essentially meaning it is a different protein on the molecular level. Secondly, the tubes in which the reactions take place are different, for the experiments with OPA and HPLC, plastic low binding tubes are used. With NMR however, glass tubes with high surface to volume ratio are used. Since they are not labeled low binding, one could expect surface adsorption and very likely an effect on heterogeneous primary nucleation of α-synuclein. Lastly, D_2O is added to the sample tube, what effect this has is not known but is another difference in solution conditions.

After allowing the sample to incubate for another 2 weeks, the sample was again measured for its apparent solubility. This is where, unexpectedly, there is an increase in monomer concentration to an average of 6.83 ±0.90 μM, measured over 24 hours. When visually inspecting the 2D spectra, the intensities are clearly higher than before. The tryptophan intensity is still roughly the same and would not account for the large increase in monomer concentration. A hypothesis is that over the 2 week incubation, there were oligomeric states that reached equilibrium, that were not present after the initial 3 day measurement. While the fibrillar structures are not visible in NMR, oligomeric states could be and these may be the reason for the increase in apparent monomer concentration.

Next, 10% DNAJB6 is added, and the dilution of the standard tryptophan is accounted for, which effectively leads to the decrease in the calculated monomer concentration, since the intensities from α-synuclein stay consistent before and after addition of DNAJB6. Over the next 3 days, the monomer concentration stays roughly the same, at the decreased level attributed to dilution. Again, the sample is incubated at 37° C for 2 weeks. When the sample is measured on again, the monomer concentration has increased. The question now is then whether this is caused by the DNAJB6 or is the same effect seen when measuring on the sample after a 2 week incubation, without addition of DNAJB6, which saw a significant increase in monomer concentration. Further experiments should be done to determine if the increase is consistent over multiple incubations, or if it is perhaps an effect only happening once, such as the formation of detectable oligomeric states.

5.5 Method development

The HPLC method development was successful in producing a protocol sensitive at the nanomolar scale. α-synuclein is clearly identifiable each time, with elution of DNAJB6 separate. An issue however is the reproducibility of the protocol. At the micromolar scale, the signal achieved is consistent between measurements of the same concentration α-synuclein, however the higher sensitivity desired, the less reproducible. The baseline "eats up" more of the signal leading to less of a peak to be integrated on. At 214 nm, which is necessary to detect low concentrations, it is also more sensitive to variations in the solvents.

Robustness is also an issue, at times the system would not give a signal at all, yet a rerun on the sample would produce the expected signal. The first run before a large batch of runs can also be strange, with wider or missing peaks, this was counteracted by running a dummy run with a small volume of α-synuclein. Also, the switching of solvents (ACN and water) would change the baseline, and the α-synuclein signal somewhat. Therefore, a new standard curve was run for each time solvents were changed. OPA fluorescence is a very robust method, with high reproducibility. It is of course not selective to any specific protein and therefore in measurements with DNAJB6, it should be accounted for. At 1% DNAJB6 it is most likely not significant, dependent on its reactivity compared to α-synuclein. A solution could be the addition of DNAJB6 to the standard curves.

6 Conclusions

- The apparent solubility of α-synuclein was determined to be 0.39 $\pm$0.016 μM, measured with OPA and 0.11 $\pm$0.013 μM, measured with HPLC.

- 1% DNAJB6 delays the aggregation of α-synuclein over the span of 837 hours. Furthermore, there could be a possible increase in solubility of α-synuclein.

- An aggregate is formed, consisting of both α-synuclein and DNAJB6, adding credence to the unhappy chaperones hypothesis, suggesting the increase in solubility for amyloid proteins in presence of chaperones, is due to the formation of co-aggregates between the amyloid protein and chaperone.

- Dis-aggregation is not detected after 837 h and there are doubts over the effectiveness of DNAJB6 at pH 5.5 for initially fibrillar system.

- NMR is viable for the measuring of α-synuclein solubility, although there are issues with discontinuous measurements. The cause of this has not yet been determined.

- HPLC is a sensitive and accurate system for the measurement of α-synuclein monomer concentration down to the nanomolars. However, it is not yet robust and reproducible enough to compare values between systems at those scales, and would therefore require further development.

7 Future work

- **Further time points** - Measuring the aggregation with DNAJB6 to determine if it is truly a reduction in aggregation and increase in solubility that occurs, or only a delay. Also, for the dis-aggregation it would be interesting to follow the reaction further, is there a delayed dis-aggregation taking place?
- **Redo at pH 8.0** - DNAJB6 is most soluble at pH 8.0, this could lead to improved dis-aggregation of α-synuclein fibrils. Unfortunately, no literary data has been found on α-synuclein aggregation at pH 8.0. Preliminary work done at pH 8.0 found it possible to form seeds at pH 8.0. The addition of these seeds however only lead to slow aggregation, and so the potency of the seeds is uncertain.
- **Different salt concentrations and temperatures** - To determine whether any discoveries for the chosen conditions in this experiment are only due to the specific system, or an inherent property of the proteins, doing the same experiments with different conditions is required.
- **Finding stoichiometry between DNAJB6 and α-synuclein** - Using multiple different concentration of DNAJB6 and determine which have an effect on the aggregation of α-synuclein as a means to find the stoichiometry between DNAJB6 and α-synuclein.
- **Determine on and off rates for amyloid fibril formation through NMR** - It has been suggested that the on and off rates for α-synuclein aggregate formation could be determined with the help of NMR. This would be interesting in the case that this is a limiting factor in the ability of DNAJB6 to disrupt these reactions, and form the co-aggregates with monomers in a system at the end state of fibrillization.
- **Follow aggregation of other amyloid protein with DNAJB6** - The unhappy chaperone hypothesis is not limited to a specific amyloid protein or a specific chaperone, so it would be of high importance to test this for multiple systems.

References

[1] Sara Linse. Toward the equilibrium and kinetics of amyloid peptide self-assembly. *Current Opinion in Structural Biology*, 70:87–98, October 2021.

[2] Werner Poewe, Klaus Seppi, Caroline M. Tanner, Glenda M. Halliday, Patrik Brundin, Jens Volkmann, Anette-Eleonore Schrag, and Anthony E. Lang. Parkinson disease. *Nature Reviews Disease Primers*, 3(1), March 2017.

[3] Tuomas P. J. Knowles, Michele Vendruscolo, and Christopher M. Dobson. The amyloid state and its association with protein misfolding diseases. *Nature Reviews Molecular Cell Biology*, 15(6):384–396, May 2014.

[4] Prince Martin, Wimo Anders, Maëlenn Guerchet, Gemma-Claire Ali, Yu-Tzu Wu, and Matthew Prina. World alzheimer report 2015 the global impact of dementia an analysis of prevalence, incidence, cost and trends. *Alzheimer's Disease International*, 2015.

[5] Pu Chun Ke, Ruhong Zhou, Louise C. Serpell, Roland Riek, Tuomas P. J. Knowles, Hilal A. Lashuel, Ehud Gazit, Ian W. Hamley, Thomas P. Davis, Marcus Fändrich, Daniel Erik Otzen, Matthew R. Chapman, Christopher M. Dobson, David S. Eisenberg, and Raffaele Mezzenga. Half a century of amyloids: past, present and future. *Chemical Society Reviews*, 49(15):5473–5509, 2020.

[6] Xiao yu Du, Xi xiu Xie, and Rui tian Liu. The role of -synuclein oligomers in parkinson's disease. *International Journal of Molecular Sciences*, 21(22):8645, November 2020.

[7] FatemehNouri Emamzadeh. Alpha-synuclein structure, functions, and interactions. *Journal of Research in Medical Sciences*, 21(1):29, 2016.

[8] F. Ulrich Hartl, Andreas Bracher, and Manajit Hayer-Hartl. Molecular chaperones in protein folding and proteostasis. *Nature*, 475(7356):324–332, July 2011.

[9] Xuechao Gao, Marta Carroni, Carmen Nussbaum-Krammer, Axel Mogk, Nadinath B. Nillegoda, Anna Szlachcic, D. Lys Guilbride, Helen R. Saibil, Matthias P. Mayer, and Bernd Bukau. Human hsp70 disaggregase reverses parkinson's-linked -synuclein amyloid fibrils. *Molecular Cell*, 59(5):781–793, September 2015.

[10] Sara Linse, Kyrre Thalberg, and Tuomas P. J. Knowles. The unhappy chaperone. *QRB Discovery*, 2, 2021.

[11] Alexander K. Buell. Stability matters, too – the thermodynamics of amyloid fibril formation. *Chemical Science*, 13(35):10177–10192, 2022.

[12] F Ulrich Hartl and Manajit Hayer-Hartl. Converging concepts of protein folding in vitro and in vivo. *Nature Structural &amp Molecular Biology*, 16(6):574–581, June 2009.

[13] Liisa Lutter, Christopher J. Serpell, Mick F. Tuite, and Wei-Feng Xue. The molecular lifecycle of amyloid – mechanism of assembly, mesoscopic organisation, polymorphism, suprastructures, and biological consequences. *Biochimica et Biophysica Acta (BBA) - Proteins and Proteomics*, 1867(11):140257, November 2019.

[14] Yaowang Li, Chunyu Zhao, Feng Luo, Zhenying Liu, Xinrui Gui, Zhipu Luo, Xiang Zhang, Dan Li, Cong Liu, and Xueming Li. Amyloid fibril structure of -synuclein determined by cryo-electron microscopy. *Cell Research*, 28(9):897–903, July 2018.

[15] Paolo Arosio, Tuomas P. J. Knowles, and Sara Linse. On the lag phase in amyloid fibril formation. *Physical Chemistry Chemical Physics*, 17(12):7606–7618, 2015.

[16] Rafaa Zeineddine and Justin J. Yerbury. The role of macropinocytosis in the propagation of protein aggregation associated with neurodegenerative diseases. *Frontiers in Physiology*, 6, October 2015.

[17] Wolfgang Hoyer, Thomas Antony, Dmitry Cherny, Gudrun Heim, Thomas M. Jovin, and Vinod Subramaniam. Dependence of -synuclein aggregate morphology on solution conditions. *Journal of Molecular Biology*, 322(2):383–393, September 2002.

[18] Mattias Törnquist, Thomas C. T. Michaels, Kalyani Sanagavarapu, Xiaoting Yang, Georg Meisl, Samuel I. A. Cohen, Tuomas P. J. Knowles, and Sara Linse. Secondary nucleation in amyloid formation. *Chemical Communications*, 54(63):8667–8684, 2018.

[19] Hilal A. Lashuel, Cassia R. Overk, Abid Oueslati, and Eliezer Masliah. The many faces of -synuclein: from structure and toxicity to therapeutic target. *Nature Reviews Neuroscience*, 14(1):38–48, December 2012.

[20] Jacqueline Burré, Manu Sharma, Theodoros Tsetsenis, Vladimir Buchman, Mark R. Etherton, and Thomas C. Südhof. -synuclein promotes SNARE-complex assembly in vivo and in vitro. *Science*, 329(5999):1663–1667, September 2010.

[21] Tim Bartels, Logan S. Ahlstrom, Avigdor Leftin, Frits Kamp, Christian Haass, Michael F. Brown, and Klaus Beyer. The n-terminus of the intrinsically disordered protein -synuclein triggers membrane binding and helix folding. *Biophysical Journal*, 99(7):2116–2124, October 2010.

[22] José Gallardo, Carmen Escalona-Noguero, and Begoña Sot. Role of -synuclein regions in nucleation and elongation of amyloid fiber assembly. *ACS Chemical Neuroscience*, 11(6):872–879, February 2020.

[23] Rina Rosenzweig, Nadinath B. Nillegoda, Matthias P. Mayer, and Bernd Bukau. The hsp70 chaperone network. *Nature Reviews Molecular Cell Biology*, 20(11):665–680, June 2019.

[24] Peter Walsh, Dejan Bursać, Yin Chern Law, Douglas Cyr, and Trevor Lithgow. The j-protein family: modulating protein assembly, disassembly and translocation. *EMBO reports*, 5(6):567–571, June 2004.

[25] Cecilia Månsson, Paolo Arosio, Rasha Hussein, Harm H. Kampinga, Reem M. Hashem, Wilbert C. Boelens, Christopher M. Dobson, Tuomas P.J. Knowles, Sara Linse, and Cecilia Emanuelsson. Interaction of the molecular chaperone DNAJB6 with growing amyloid-beta 42 (a42) aggregates leads to sub-stoichiometric inhibition of amyloid formation. *Journal of Biological Chemistry*, 289(45):31066–31076, November 2014.

[26] Vaishali Kakkar, Cecilia Månsson, Eduardo P. de Mattos, Steven Bergink, Marianne van der Zwaag, Maria A.W.H. van Waarde, Niels J. Kloosterhuis, Ronald Melki, Remco T.P. van Cruchten, Salam Al-Karadaghi, Paolo Arosio, Christopher M. Dobson, Tuomas P.J. Knowles, Gillian P. Bates, Jan M. van Deursen, Sara Linse, Bart van de Sluis, Cecilia Emanuelsson, and Harm H. Kampinga. The s/t-rich motif in the DNAJB6 chaperone delays polyglutamine aggregation and the onset of disease in a mouse model. *Molecular Cell*, 62(2):272–283, April 2016.

[27] Cecilia Månsson, Remco T. P. van Cruchten, Ulrich Weininger, Xiaoting Yang, Risto Cukalevski, Paolo Arosio, Christopher M. Dobson, Tuomas Knowles, Mikael Akke, Sara Linse, and Cecilia Emanuelsson. Conserved s/t residues of the human chaperone DNAJB6 are required for effective inhibition of a42 amyloid fibril formation. *Biochemistry*, 57(32):4891–4902, July 2018.

[28] Ricardo Gaspar, Georg Meisl, Alexander K. Buell, Laurence Young, Clemens F. Kaminski, Tuomas P. J. Knowles, Emma Sparr, and Sara Linse. Secondary nucleation of monomers on fibril surface dominatesi/i-synuclein aggregation and provides autocatalytic amyloid amplification. *Quarterly Reviews of Biophysics*, 50, 2017.

[29] Thermofisher, fluoraldehydetm o-phthaldialdehyde reagent solution (opa). https://www.thermofisher.com/order/catalog/product/26025. [Online] Accessed: 2023-06-11.

[30] Mbl life science, the principle and method of polyacrylamide gel electrophoresis (sds-page). https://ruo.mbl.co.jp/bio/e/support/method/sds-page.html. [Online] Accessed: 2023-06-11.

[31] Kseniia Afitska, Anna Fucikova, Volodymyr V. Shvadchak, and Dmytro A. Yushchenko. -synuclein aggregation at low concentrations. *Biochimica et Biophysica Acta (BBA) - Proteins and Proteomics*, 1867(7-8):701–709, July 2019.

Appendix

A1. OPA fluorescence standard curve

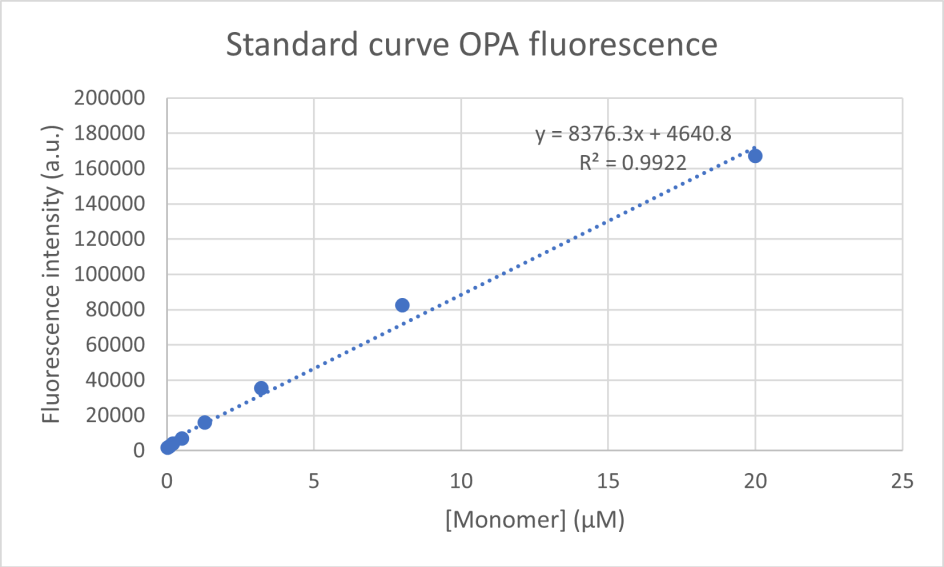

Figure 25: Standard curve measured with OPA fluorescence for monomeric α-synuclein, with 3 replicates and 8 concentrations between 20 μM and 0.03 μM.

A2. Dis-aggregation

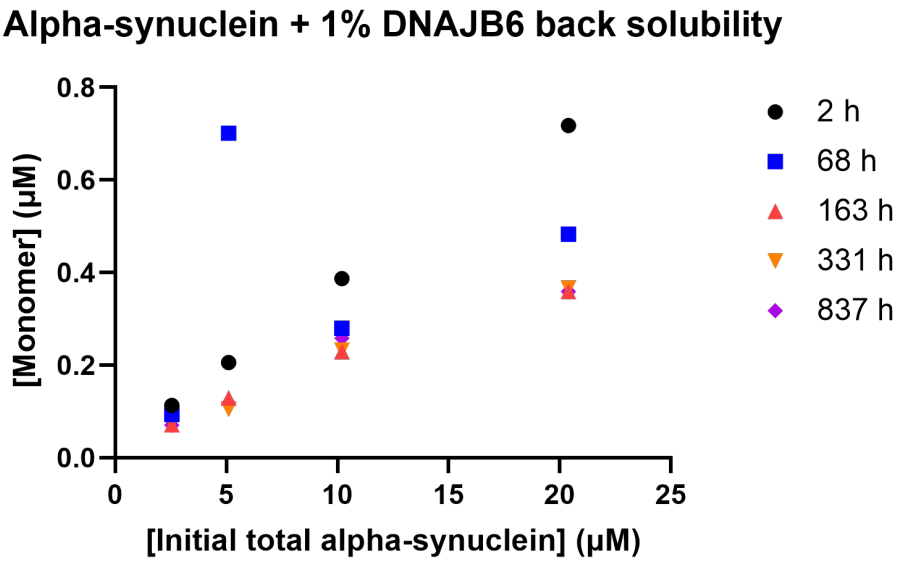

Figure 26: Monomer concentration against initial total α-synuclein concentration at different time points for α-synuclein dis-aggregation at pH 5.5 with 1% DNAJB6, measured with OPA fluorescence.